Supporting Information

Mixed Chelating Ligands Used to Regulate the Luminescence of Ln(III) Complexes and Single-Ion Magnet Behavior in Dy-based Analogues

Hai-Ling Wang,[1,⊥] Xiong-Feng Ma,[1,⊥] Hua-Hong Zou, *[,1] Kai Wang,[3] Bo Li*,[2] Zi-Lu Chen,[1] Fu-Pei Liang*[,1,3]

[1]State Key Laboratory for Chemistry and Molecular Engineering of Medicinal Resources, School of Chemistry & Pharmacy of Guangxi Normal University, Guilin 541004, P. R. China. E-mail: fliangoffice@yahoo.com, gxnuchem@foxmail.com

[2]College of Chemistry and Pharmaceutical Engineering, Nanyang Normal University, Nanyang 473061, P. R. China. E-mail: libozzu0107@163.com

[3]Guangxi Key Laboratory of Electrochemical and Magnetochemical Functional Materials, College of Chemistry and Bioengineering, Guilin University of Technology, Guilin 541004, P. R. China

	complexes.
Figure S1	Complexes **1-11** thermogravimetric curves (a-j, TG and DTG).
Figure S2	PXRD testing and fitting of complexes **1-11** (a-j).
Figure S3	Ligands $\mathbf{L^1}$, $\mathbf{L^2}$, $\mathbf{L^3}$ were dissolved in DMF by UV-vis absorption spectroscopy.
Figure S4	UV-visible absorption spectrum of complex **3** in DMF solution.
Figure S5	Ligands $\mathbf{L^1}$, $\mathbf{L^2}$, and $\mathbf{L^3}$ were fluorescently resolved in DMF.
Figure S6	Fluorescence spectra of complex **3** in DMF solution.
Figure S7	Complexes **3**, **5**, **9-11** solid fluorescence test pattern.
Figure S8	ESI-MS spectra of **3** in DMF (In-Source CID 0 eV).
Figure S9	The superposed simulated and observed spectra of several species for **3**.
Figure S10	Positive ESI-MS spectra of **5-7** and **9-11** in DMF (In-Source CID 0 eV).
Figure S11-16	The superposed simulated and observed spectra of several species for **5-7** and **9-11** in positive mode.
Figure S17	Negative ESI-MS spectra of **5-7** and **9-11** in DMF (In-Source CID 0 eV).
Figure S18-23	The superposed simulated and observed spectra of several species for **5-7** and **9-11** in negative mode.
Figure S24	Temperature dependence of $\chi_m T$ for **1-4**, and **8**.
Figure S25	Fitting C and θ of $1/\chi$ for **1-4** and **8**.
Figure S26	Field dependence of the magnetization for (a) **1**, (b) **2**, (c) **4**, (d) **8** and (e) **3**.
Figure S27	Variable-frequency dependent ac susceptibilities under 1500 Oe field for **1** (a and b), **2** (g and h) and **11** (j and k). Variable-frequency dependent ac susceptibilities under 0 Oe field for **2**. (d and e), cole-cole plots for **1** (c), **2** (i) and **11** (l) under 1500 Oe dc field, and cole-cole plots for **2** (f) under 0 Oe dc field.

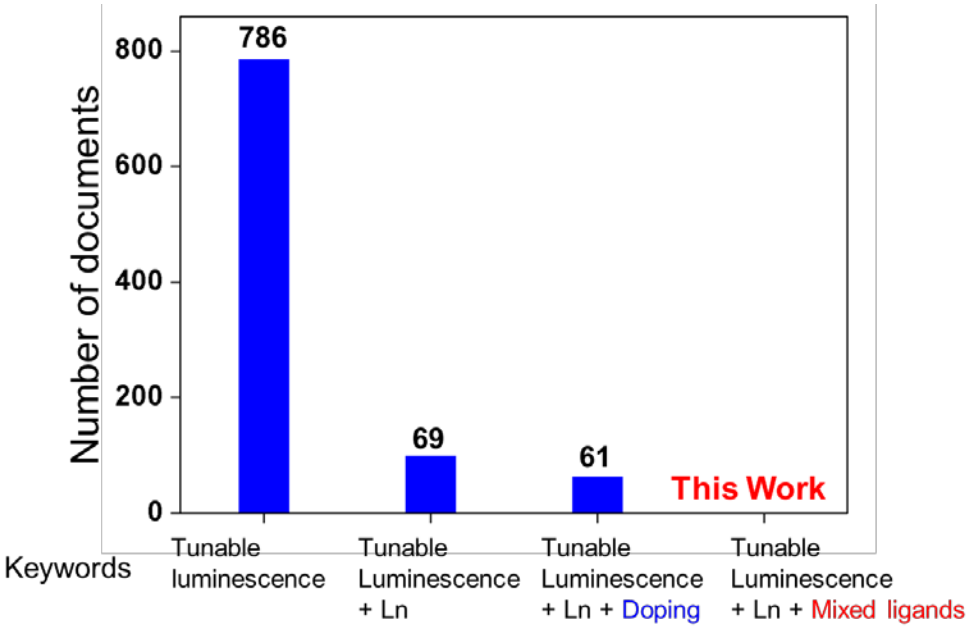

Scheme S1. SciFinder queries methods and literature for modulating Luminescence of Ln(III) complexes.

Table S1. Crystallographic data of the complexes **1**-**6**.

Complex	**1**	**2**	**3**	**4**	**5**	**6**
Formula	$C_{123}H_{82}Br_{24}Cl_9Dy_4N_{12}O_{16}$	$C_{24}H_{16}DyN_7O_9$	$C_{30}H_{20}Cl_6DyN_3O_4$	$C_{32}H_{20}Br_4DyN_5O_5$	$C_{32}H_{20}Br_4HoN_5O_5$	$C_{32}H_{20}Br_4ErN_5O_5$
Formula weight	4870.90	708.94	861.69	1036.67	1039.10	1041.43
T (K)	293(2)	293(2)	296.15	296.15	293(2)	296.15
Crystal system	Triclinic	Monoclinic	Monoclinic	Monoclinic	Monoclinic	Monoclinic
Space group	*P*-1	*C*2/*c*	*C*2/*c*	*P*2$_1$/*c*	*P*2$_1$/*c*	*P*2$_1$/*c*
a (Å)	13.3670(4)	11.145(3)	28.994(8)	13.583(3)	13.5558(2)	13.552(4)
b (Å)	13.7483(4)	17.878(3)	10.646(3)	16.809(4)	16.7642(2)	16.758(5)
c (Å)	20.9730(6)	13.003(3)	23.517(7)	14.442(3)	14.3978(2)	14.397(4)
α (°)	71.835(3)	90.00	90.00	90.00	90.00	90.00
β (°)	79.055(3)	100.47(2)	119.288(5)	97.666(4)	97.6210(10)	97.625(4)
γ (°)	86.694(3)	90.00	90.00	90.00	90.00	90.00
V (Å^3)	3595.59(19)	2547.9(1)	6331(3)	3267.7(12)	3243.03(8)	3240.6(15)
Z	1	4	8	4	4	4
D_c (g cm^{-3})	2.250	1.848	1.808	2.107	2.128	2.135

μ (mm^{-1})	20.809	3.001	2.908	7.227	7.418	7.572
Reflns coll.	42056	9332	17782	39265	21530	39105
Unique reflns	14202	2497	6306	6658	5687	6619
R_{int}	0.042	0.027	0.046	0.061	0.026	0.042
$^{a}R_1$ [I ≥ 2σ(I)]	0.048	0.021	0.038	0.030	0.024	0.025
$^{b}wR_2$ (all data)	0.129	0.045	0.110	0.077	0.052	0.062
GOF	1.038	1.097	1.021	1.021	1.043	1.039

Table S2. Crystallographic data of the complexes **7**-**11**.

Complex	**7**	**8**	**9**	**10**	**11**
Formula	$C_{32}H_{20}Br_4TbN_5O_5$	$C_{32}H_{20}Cl_4DyN_5O_5$	$C_{32}H_{20}Cl_4HoN_5O_5$	$C_{32}H_{20}Cl_4ErN_5O_5$	$C_{32}H_{20}Cl_4TbN_5O_5$
Formula weight	1033.09	858.83	861.26	863.59	855.25
T (K)	296.15	150.0	296.15	293(2)	296.15
Crystal system	Monoclinic	Monoclinic	Monoclinic	Monoclinic	Monoclinic
Space group	$P2_1/c$	$P2_1/c$	$P2_1/c$	$P2_1/c$	$P2_1/c$
a (Å)	13.5432(11)	13.0622(6)	13.2312(18)	13.2305(3)	13.221(3)
b (Å)	16.8109(13)	16.6648(8)	16.689(2)	16.6540(3)	16.762(4)
c (Å)	14.4543(11)	14.2828(6)	14.3530(19)	14.3223(3)	14.398(3)
α (°)	90.00	90.00	90.00	90.00	90.00
β (°)	97.5140(10)	97.7270(10)	97.769(2)	97.802(2)	97.620(4)
γ (°)	90.00	90.00	90.00	90.00	90.00
V (Å^3)	3262.6(4)	3080.8(2)	3140.3(7)	3126.57(11)	3162.6(13)
Z	4	4	4	4	4
D_c.(g cm^{-3})	2.103	1.852	1.822	1.835	1.796
μ (mm^{-1})	7.116	2.824	2.911	3.077	2.625
Reflns coll.	39266	50449	37976	22262	29050
Unique reflns	6691	6328	6486	6131	6540
R_{int}	0.045	0.067	0.034	0.025	0.026
$^{a}R_1$ [I ≥ 2σ(I)]	0.028	0.028	0.022	0.024	0.025

$^{b}wR_2$ (all data)	0.062	0.062	0.064	0.053	0.071
GOF	1.008	1.078	1.054	1.040	1.023

Table S3. Selected bond lengths (Å) and angles (°) of the complexes.

1					
Dy1—O5	2.250 (4)	Dy1—N2	2.600 (5)	Dy1—O7	2.200 (4)
Dy1—O6	2.250 (4)	Dy1—N3	2.592 (5)	Dy1—O8	2.354 (4)
Dy1—N1	2.610 (5)				
O5—Dy1—O6	82.47 (14)	O7—Dy1—N3	66.63 (15)	O6—Dy1—N2	146.58 (17)
O5—Dy1—O8	90.30 (14)	O8—Dy1—N1	74.48 (14)	O6—Dy1—N3	86.11 (14)
O5—Dy1—N1	144.65 (15)	O8—Dy1—N2	77.38 (15)	O7—Dy1—O5	131.33 (16)
O5—Dy1—N2	66.56 (17)	O8—Dy1—N3	176.09 (15)	O7—Dy1—O6	131.70 (15)
O5—Dy1—N3	86.64 (14)	N2—Dy1—N1	136.48 (18)	O7—Dy1—O8	117.27 (15)
O6—Dy1—O8	91.09 (14)	N3—Dy1—N1	106.77 (14)	O7—Dy1—N1	83.57 (16)
O6—Dy1—N1	66.49 (15)	N3—Dy1—N2	103.56 (15)	O7—Dy1—N2	80.62 (18)
Symmetry code: (i) -*x*+1, -*y*-1, -*z*+1.					
2					
Dy1—O1	2.525 (2)	Dy1—O4	2.463 (2)	Dy1—N3^{i}	2.919 (3)
Dy1—O2	2.4598 (19)	Dy1—N2	2.499 (2)	Dy1—N1	2.559 (2)
Dy1—N4	2.882 (4)				
O1^{i}—Dy1—O1	171.74 (9)	O2^{i}—Dy1—N1^{i}	75.27 (7)	O4—Dy1—N1	136.60 (7)
O1^{i}—Dy1—N3^{i}	25.51 (7)	O2—Dy1—N1^{i}	141.54 (7)	O4—Dy1—N4	25.87 (6)
O1—Dy1—N3^{i}	150.65 (7)	O2—Dy1—N1	75.27 (7)	N2—Dy1—O1	113.55 (7)
O1—Dy1—N1^{i}	118.37 (7)	O2—Dy1—N4	71.49 (5)	N2—Dy1—O1^{i}	69.25 (7)
O1—Dy1—N1	69.19 (7)	O4^{i}—Dy1—O1^{i}	67.60 (7)	N2—Dy1—N2^{i}	143.35 (10)
O1—Dy1—N4	85.87 (4)	O4—Dy1—O1^{i}	104.57 (7)	N2^{i}—Dy1—N3^{i}	92.97 (7)

O2—Dy1—O1^{i}	125.54 (7)	O4—Dy1—O1	67.60 (7)	N2—Dy1—N3^{i}	94.76 (7)
O2—Dy1—O1	51.18 (6)	O4^{i}—Dy1—O4	51.74 (11)	N2^{i}—Dy1—N1	84.20 (7)
O2^{i}—Dy1—O2	142.98 (10)	O4—Dy1—N2^{i}	84.38 (8)	N2—Dy1—N1	65.01 (7)
O2—Dy1—O4	74.98 (7)	O4—Dy1—N2	131.58 (8)	N2—Dy1—N4	108.32 (5)
O2^{i}—Dy1—O4	71.81 (7)	N4—Dy1—N3^{i}	77.62 (5)	N1^{i}—Dy1—N3^{i}	70.17 (7)
O2—Dy1—N2^{i}	120.42 (7)	O4—Dy1—N3^{i}	88.18 (7)	N1—Dy1—N3^{i}	134.13 (7)
O2—Dy1—N2	72.14 (7)	O4^{i}—Dy1—N3^{i}	69.27 (7)	N1^{i}—Dy1—N1	67.26 (10)
O2—Dy1—N3^{i}	139.93 (6)	O4—Dy1—N1^{i}	140.52 (7)	N1—Dy1—N4	146.37 (5)
O2^{i}—Dy1—N3^{i}	25.67 (6)				
Symmetry code: (i) -*x*+1, *y*, -*z*+3/2.					
3					
Dy1—O1	2.243 (4)	Dy1—O3	2.225 (4)	Dy1—N1	2.607 (5)
Dy1—O2	2.204 (4)	Dy1—O4	2.337 (4)	Dy1—N2	2.608 (5)
Dy1—N3	2.624 (4)				
O1—Dy1—O4	93.00 (15)	O2—Dy1—N1	82.21 (16)	O3—Dy1—N3	66.85 (14)
O1—Dy1—N1	66.39 (16)	O2—Dy1—N2	66.46 (16)	O4—Dy1—N1	81.51 (15)
O1—Dy1—N2	89.87 (16)	O2—Dy1—N3	81.46 (15)	O4—Dy1—N2	176.46 (14)
O1—Dy1—N3	141.61 (15)	O3—Dy1—O1	78.51 (14)	O4—Dy1—N3	73.57 (14)
O2—Dy1—O1	136.14 (16)	O3—Dy1—O4	93.08 (15)	N1—Dy1—N2	101.56 (15)
O2—Dy1—O3	131.60 (15)	O3—Dy1—N1	144.02 (15)	N1—Dy1—N3	142.00 (15)
O2—Dy1—O4	112.51 (15)	O3—Dy1—N2	85.47 (16)	N2—Dy1—N3	102.90 (15)
4					
Dy1—O1	2.201 (3)	Dy1—N3	2.652 (4)	Dy1—N1	2.538 (4)
Dy1—O2	2.208 (3)	Dy1—N4	2.624 (3)	Dy1—N5	2.894 (4)
Dy1—O4	2.509 (3)	Dy1—N2	2.546 (3)	Dy1—O3	2.426 (4)
O1—Dy1—O2	131.85 (12)	O2—Dy1—N1	143.90 (11)	N2—Dy1—N4	141.92 (10)

O1—Dy1—O4	82.04 (11)	O2—Dy1—N5	108.21 (12)	N2—Dy1—N5	90.42 (12)
O1—Dy1—N3	66.57 (10)	O2—Dy1—O3	87.92 (12)	N1—Dy1—N3	84.31 (11)
O1—Dy1—N4	84.93 (11)	O4—Dy1—N3	144.16 (11)	N1—Dy1—N4	146.09 (11)
O1—Dy1—N2	132.17 (11)	O4—Dy1—N4	76.60 (11)	N1—Dy1—N2	64.98 (11)
O1—Dy1—N1	78.04 (11)	O4—Dy1—N2	111.98 (11)	N1—Dy1—N5	72.84 (12)
O1—Dy1—N5	107.09 (12)	O4—Dy1—N1	72.18 (11)	O3—Dy1—O4	51.50 (12)
O1—Dy1—O3	132.76 (12)	O4—Dy1—N5	25.69 (10)	O3—Dy1—N3	150.17 (12)
O2—Dy1—O4	124.40 (11)	N3—Dy1—N5	157.15 (11)	O3—Dy1—N4	91.20 (12)
O2—Dy1—N3	90.44 (11)	N4—Dy1—N3	115.44 (11)	O3—Dy1—N2	70.38 (12)
O2—Dy1—N4	67.01 (10)	N4—Dy1—N5	84.72 (11)	O3—Dy1—N1	79.69 (12)
O2—Dy1—N2	78.93 (11)	N2—Dy1—N3	80.07 (11)	O3—Dy1—N5	25.90 (11)
5					
Ho1—O1	2.194 (2)	Ho1—N4	2.608 (3)	Ho1—N1	2.514 (3)
Ho1—O2	2.193 (2)	Ho1—N2	2.525 (3)	Ho1—O3	2.407 (3)
Ho1—O4	2.488 (3)	Ho1—N3	2.641 (3)	Ho1—N5	2.871 (3)
O1—Ho1—O4	82.11 (9)	O2—Ho1—N1	143.95 (9)	N2—Ho1—N5	90.61 (9)
O1—Ho1—N4	84.35 (8)	O2—Ho1—O3	88.13 (10)	N3—Ho1—N5	157.64 (9)
O1—Ho1—N2	132.47 (9)	O2—Ho1—N5	108.31 (10)	N1—Ho1—N4	146.06 (9)
O1—Ho1—N3	66.89 (9)	O4—Ho1—N4	76.50 (9)	N1—Ho1—N2	64.96 (9)
O1—Ho1—N1	78.44 (9)	O4—Ho1—N2	112.13 (9)	N1—Ho1—N3	84.48 (9)
O1—Ho1—O3	132.96 (9)	O4—Ho1—N3	144.53 (8)	N1—Ho1—N5	73.16 (9)
O1—Ho1—N5	107.29 (10)	O4—Ho1—N1	72.34 (9)	O3—Ho1—O4	51.57 (9)
O2—Ho1—O1	131.25 (9)	O4—Ho1—N5	25.74 (9)	O3—Ho1—N4	91.28 (10)
O2—Ho1—O4	124.60 (9)	N4—Ho1—N3	115.22 (8)	O3—Ho1—N2	70.48 (10)
O2—Ho1—N4	67.17 (8)	N4—Ho1—N5	84.58 (9)	O3—Ho1—N3	150.14 (10)
O2—Ho1—N2	78.99 (9)	N2—Ho1—N4	142.13 (8)	O3—Ho1—N1	79.84 (10)

O2—Ho1—N3	89.83 (9)	N2—Ho1—N3	79.88 (9)	O3—Ho1—N5	25.89 (9)
6					
Er1—O1	2.184 (2)	Er1—N4	2.602 (3)	Er1—N1	2.498 (3)
Er1—O2	2.183 (2)	Er1—N2	2.514 (3)	Er1—O3	2.397 (3)
Er1—O4	2.481 (3)	Er1—N3	2.631 (3)	Er1—N5	2.855 (4)
O1—Er1—O4	81.97 (9)	O2—Er1—N1	144.10 (9)	N2—Er1—N5	90.83 (10)
O1—Er1—N4	83.89 (9)	O2—Er1—O3	87.92 (11)	N3—Er1—N5	158.05 (9)
O1—Er1—N2	132.84 (9)	O2—Er1—N5	108.28 (11)	N1—Er1—N4	145.86 (9)
O1—Er1—N3	67.13 (9)	O4—Er1—N4	76.27 (9)	N1—Er1—N2	65.24 (9)
O1—Er1—N1	78.54 (10)	O4—Er1—N2	112.40 (9)	N1—Er1—N3	84.52 (9)
O1—Er1—O3	133.22 (10)	O4—Er1—N3	144.66 (9)	N1—Er1—N5	73.53 (10)
O1—Er1—N5	107.34 (10)	O4—Er1—N1	72.48 (9)	O3—Er1—O4	51.85 (10)
O2—Er1—O1	130.91 (10)	O4—Er1—N5	25.87 (9)	O3—Er1—N4	91.02 (10)
O2—Er1—O4	124.73 (10)	N4—Er1—N3	115.13 (9)	O3—Er1—N2	70.62 (10)
O2—Er1—N4	67.37 (9)	N4—Er1—N5	84.31 (9)	O3—Er1—N3	150.29 (10)
O2—Er1—N2	78.86 (9)	N2—Er1—N4	142.18 (9)	O3—Er1—N1	80.42 (11)
O2—Er1—N3	89.50 (9)	N2—Er1—N3	79.84 (9)	O3—Er1—N5	26.06 (10)
7					
Tb1—O1	2.211 (2)	Tb1—N4	2.627 (3)	Tb1—N1	2.542 (3)
Tb1—O2	2.213 (3)	Tb1—N2	2.551 (3)	Tb1—N5	2.898 (4)
Tb1—O4	2.515 (3)	Tb1—N3	2.663 (3)	Tb1—O3	2.435 (3)
O1—Tb1—O2	132.02 (10)	O2—Tb1—N1	143.55 (10)	N2—Tb1—N5	90.05 (11)
O1—Tb1—O4	82.38 (10)	O2—Tb1—N5	107.78 (11)	N3—Tb1—N5	157.10 (10)
O1—Tb1—N4	85.23 (9)	O2—Tb1—O3	87.73 (11)	N1—Tb1—N4	146.69 (10)
O1—Tb1—N2	131.86 (10)	O4—Tb1—N4	77.03 (10)	N1—Tb1—N2	64.42 (10)
O1—Tb1—N3	66.31 (9)	O4—Tb1—N2	111.55 (10)	N1—Tb1—N3	84.10 (10)

O1—Tb1—N1	78.19 (10)	O4—Tb1—N3	144.14 (10)	N1—Tb1—N5	73.00 (10)
O1—Tb1—N5	107.50 (11)	O4—Tb1—N1	72.31 (10)	O3—Tb1—O4	51.23 (10)
O1—Tb1—O3	132.83 (10)	O4—Tb1—N5	25.75 (10)	O3—Tb1—N4	91.24 (11)
O2—Tb1—O4	124.17 (10)	N4—Tb1—N3	115.34 (9)	O3—Tb1—N2	70.36 (11)
O2—Tb1—N4	66.70 (9)	N4—Tb1—N5	85.00 (10)	O3—Tb1—N3	150.24 (11)
O2—Tb1—N2	79.14 (10)	N2—Tb1—N4	141.91 (9)	O3—Tb1—N1	79.68 (11)
O2—Tb1—N3	90.76 (10)	N2—Tb1—N3	80.16 (10)	O3—Tb1—N5	25.56 (10)
8					
Dy1—O1	2.201 (2)	Dy1—N1	2.530 (3)	Dy1—O3	2.426 (3)
Dy1—O2	2.202 (2)	Dy1—N3	2.640 (3)	Dy1—N2	2.533 (3)
Dy1—O4	2.508 (3)	Dy1—N4	2.619 (3)	Dy1—N5	2.894 (3)
O1—Dy1—O2	132.45 (9)	O2—Dy1—O3	89.12 (9)	N3—Dy1—N5	153.85 (8)
O1—Dy1—O4	81.06 (8)	O2—Dy1—N2	78.01 (9)	N4—Dy1—N3	117.24 (9)
O1—Dy1—N1	78.25 (9)	O2—Dy1—N5	109.73 (9)	N4—Dy1—N5	86.14 (8)
O1—Dy1—N3	67.12 (9)	O4—Dy1—N1	72.29 (9)	O3—Dy1—O4	51.75 (8)
O1—Dy1—N4	85.33 (9)	O4—Dy1—N3	142.73 (8)	O3—Dy1—N1	78.18 (9)
O1—Dy1—O3	131.74 (9)	O4—Dy1—N4	77.06 (8)	O3—Dy1—N3	147.86 (9)
O1—Dy1—N2	132.28 (9)	O4—Dy1—N2	112.63 (9)	O3—Dy1—N4	92.38 (9)
O1—Dy1—N5	106.03 (9)	O4—Dy1—N5	25.91 (8)	O3—Dy1—N2	70.04 (9)
O2—Dy1—O4	125.42 (8)	N1—Dy1—N3	82.33 (9)	O3—Dy1—N5	25.99 (8)
O2—Dy1—N1	142.75 (9)	N1—Dy1—N4	147.02 (9)	N2—Dy1—N3	78.61 (9)
O2—Dy1—N3	91.20 (9)	N1—Dy1—N2	64.74 (9)	N2—Dy1—N4	141.31 (8)
O2—Dy1—N4	67.20 (9)	N1—Dy1—N5	71.51 (9)	N2—Dy1—N5	90.27 (9)
9					
Ho1—O1	2.1946 (19)	Ho1—N1	2.521 (2)	Ho1—N2	2.524 (2)
Ho1—O2	2.1895 (19)	Ho1—N4	2.618 (2)	Ho1—O3	2.416 (2)

Ho1—O4	2.492 (2)	Ho1—N3	2.633 (2)	Ho1—N5	2.879 (3)
O1—Ho1—O4	81.91 (7)	O2—Ho1—N2	78.38 (7)	N4—Ho1—N3	115.79 (7)
O1—Ho1—N1	78.49 (8)	O2—Ho1—O3	89.07 (8)	N4—Ho1—N5	86.16 (7)
O1—Ho1—N4	84.29 (7)	O2—Ho1—N5	109.46 (9)	N3—Ho1—N5	155.48 (8)
O1—Ho1—N3	67.05 (7)	O4—Ho1—N1	72.46 (7)	N2—Ho1—N4	141.76 (7)
O1—Ho1—N2	132.72 (7)	O4—Ho1—N4	77.13 (7)	N2—Ho1—N3	79.17 (7)
O1—Ho1—O3	132.50 (8)	O4—Ho1—N3	143.86 (7)	N2—Ho1—N5	90.17 (7)
O1—Ho1—N5	106.98 (8)	O4—Ho1—N2	112.36 (7)	O3—Ho1—O4	51.44 (8)
O2—Ho1—O1	131.23 (8)	O4—Ho1—N5	25.86 (7)	O3—Ho1—N1	79.16 (8)
O2—Ho1—O4	125.20 (8)	N1—Ho1—N4	146.75 (7)	O3—Ho1—N4	92.36 (8)
O2—Ho1—N1	143.50 (7)	N1—Ho1—N3	83.23 (7)	O3—Ho1—N3	148.94 (8)
O2—Ho1—N4	67.21 (7)	N1—Ho1—N2	65.12 (7)	O3—Ho1—N2	70.26 (8)
O2—Ho1—N3	90.12 (8)	N1—Ho1—N5	72.25 (8)	O3—Ho1—N5	25.72 (8)
10					
Er1—O1	2.1795 (19)	Er1—N4	2.606 (2)	Er1—N3	2.624 (2)
Er1—O2	2.1809 (19)	Er1—N1	2.504 (2)	Er1—O3	2.398 (2)
Er1—O4	2.484 (2)	Er1—N2	2.505 (2)	Er1—N5	2.868 (3)
O1—Er1—O2	130.93 (8)	O2—Er1—N3	89.74 (8)	N1—Er1—N3	83.54 (7)
O1—Er1—O4	81.74 (7)	O2—Er1—O3	88.89 (8)	N1—Er1—N5	72.37 (8)
O1—Er1—N4	83.84 (7)	O2—Er1—N5	109.43 (8)	N2—Er1—N4	141.78 (7)
O1—Er1—N1	78.72 (8)	O4—Er1—N4	76.90 (7)	N2—Er1—N3	79.03 (7)
O1—Er1—N2	133.10 (7)	O4—Er1—N1	72.41 (7)	N2—Er1—N5	90.47 (8)
O1—Er1—N3	67.36 (7)	O4—Er1—N2	112.74 (7)	N3—Er1—N5	155.91 (7)
O1—Er1—O3	132.74 (8)	O4—Er1—N3	144.05 (7)	O3—Er1—O4	51.75 (8)
O1—Er1—N5	107.02 (8)	O4—Er1—N5	26.00 (7)	O3—Er1—N4	92.16 (8)
O2—Er1—O4	125.34 (8)	N4—Er1—N3	115.69 (7)	O3—Er1—N1	79.42 (8)

O2—Er1—N4	67.41 (7)	N4—Er1—N5	85.89 (7)	O3—Er1—N2	70.42 (8)
O2—Er1—N1	143.63 (7)	N1—Er1—N4	146.44 (7)	O3—Er1—N3	149.03 (8)
O2—Er1—N2	78.18 (7)	N1—Er1—N2	65.46 (7)	O3—Er1—N5	25.89 (7)
11					
Tb1—O1	2.215 (2)	Tb1—N4	2.641 (3)	Tb1—N2	2.545 (3)
Tb1—O2	2.215 (2)	Tb1—O4	2.519 (2)	Tb1—O3	2.448 (3)
Tb1—N1	2.549 (3)	Tb1—N3	2.659 (3)	Tb1—N5	2.908 (3)
O1—Tb1—N1	78.67 (8)	O2—Tb1—N2	78.37 (8)	O4—Tb1—N5	25.59 (8)
O1—Tb1—N4	85.04 (8)	O2—Tb1—O3	88.74 (9)	N3—Tb1—N5	154.86 (8)
O1—Tb1—O4	82.35 (8)	O2—Tb1—N5	109.02 (9)	N2—Tb1—N1	64.36 (8)
O1—Tb1—N3	66.47 (8)	N1—Tb1—N4	147.66 (8)	N2—Tb1—N4	141.54 (8)
O1—Tb1—N2	132.17 (8)	N1—Tb1—N3	82.74 (8)	N2—Tb1—N3	79.21 (8)
O1—Tb1—O3	132.38 (8)	N1—Tb1—N5	72.12 (8)	N2—Tb1—N5	89.94 (8)
O1—Tb1—N5	107.10 (9)	N4—Tb1—N3	115.96 (8)	O3—Tb1—N1	78.78 (9)
O2—Tb1—O1	131.93 (9)	N4—Tb1—N5	86.54 (8)	O3—Tb1—N4	92.44 (9)
O2—Tb1—N1	142.72 (8)	O4—Tb1—N1	72.61 (8)	O3—Tb1—O4	50.94 (8)
O2—Tb1—N4	66.80 (8)	O4—Tb1—N4	77.71 (8)	O3—Tb1—N3	148.89 (9)
O2—Tb1—O4	124.72 (8)	O4—Tb1—N3	143.53 (8)	O3—Tb1—N2	70.29 (9)
O2—Tb1—N3	91.07 (8)	O4—Tb1—N2	111.89 (8)	O3—Tb1—N5	25.50 (8)

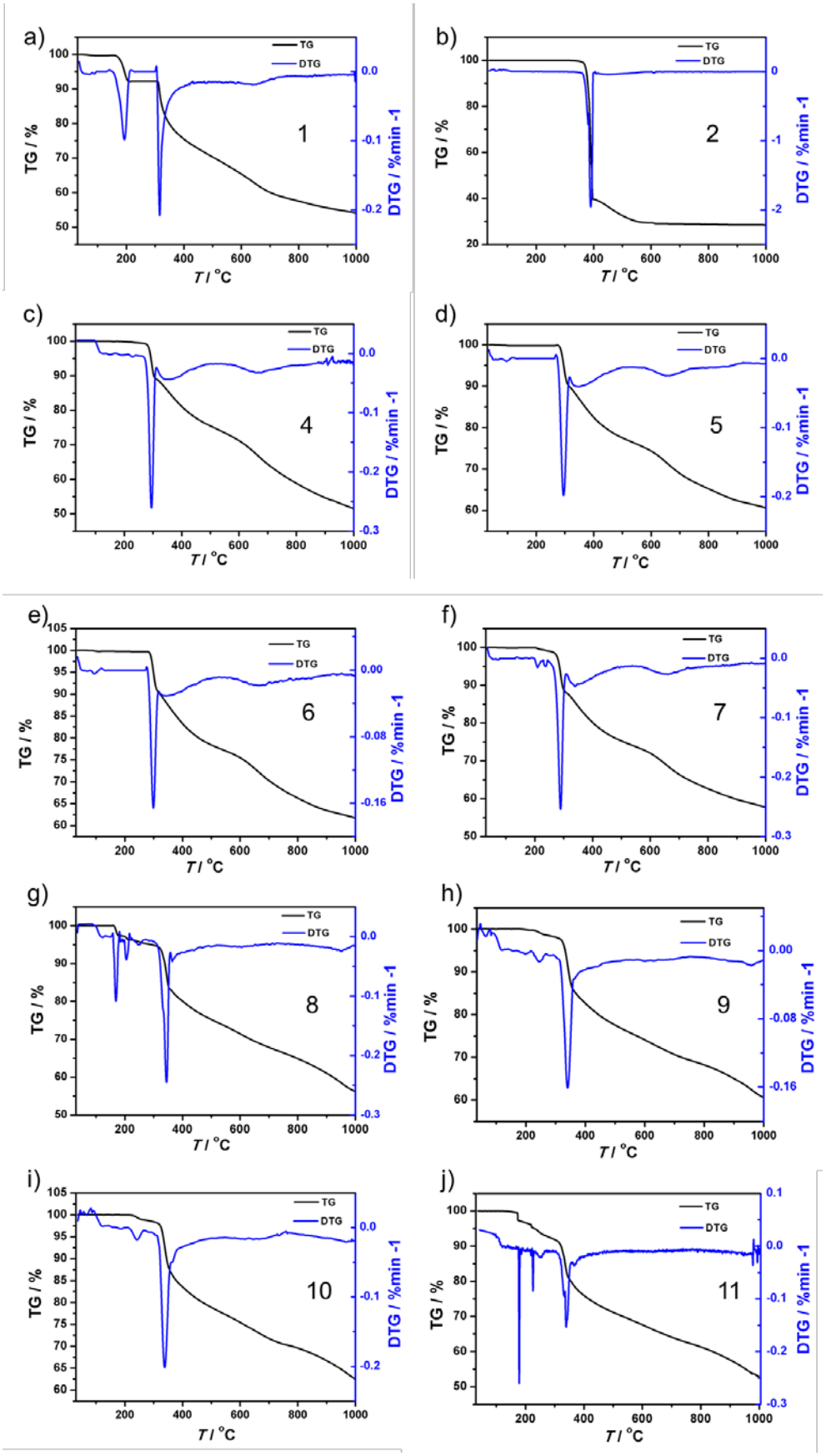

Figure S1. Complexes **1-11** thermogravimetric curves (a-j, TG and DTG).

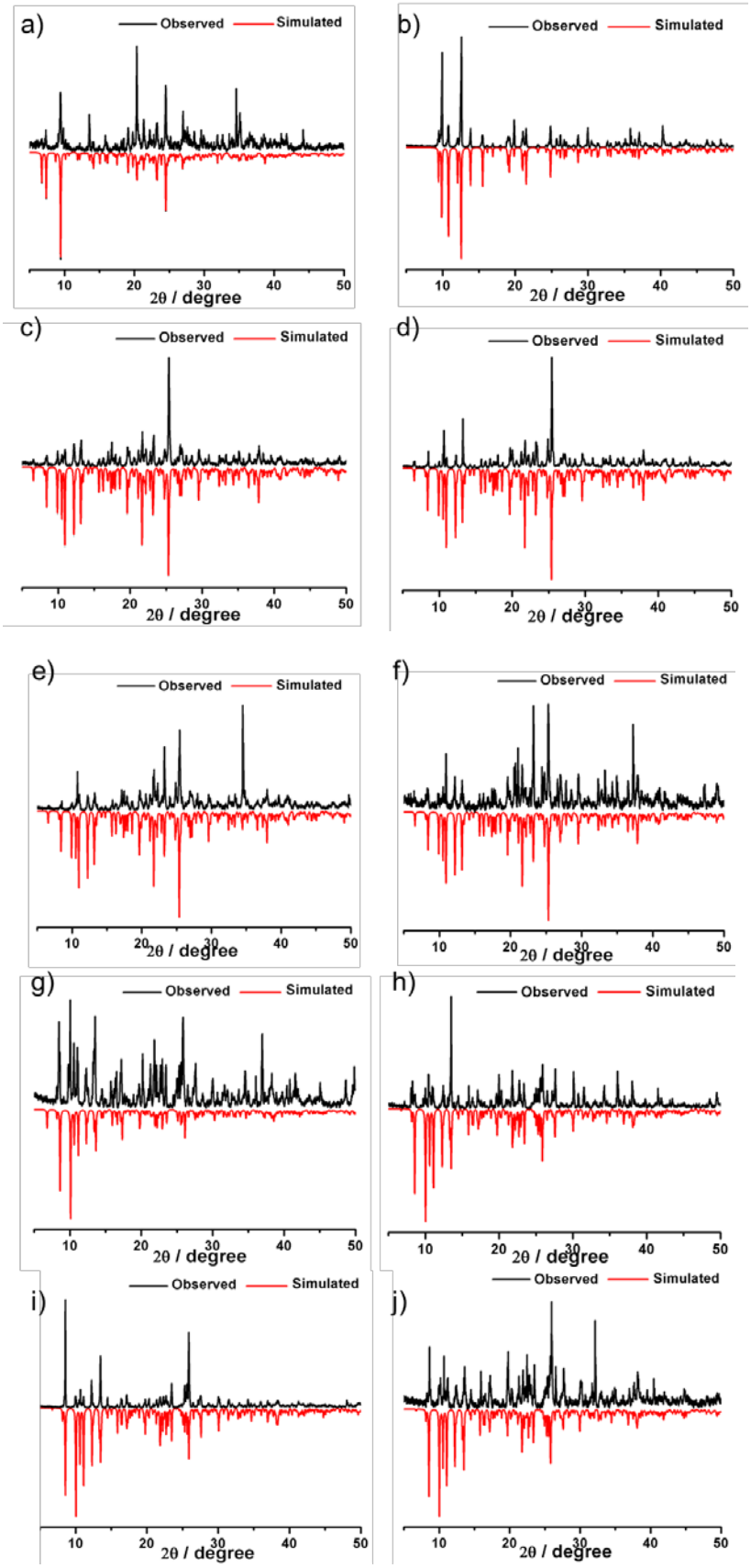

Figure S2. PXRD testing and fitting of complexes **1**-**11** (a-j).

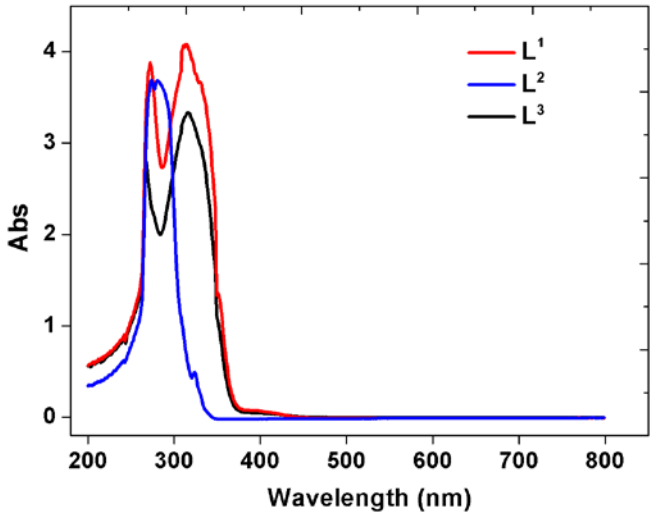

Figure S3. Ligands **L**^{1}, **L**^{2}, **L**^{3} were dissolved in DMF by UV-vis absorption spectroscopy.

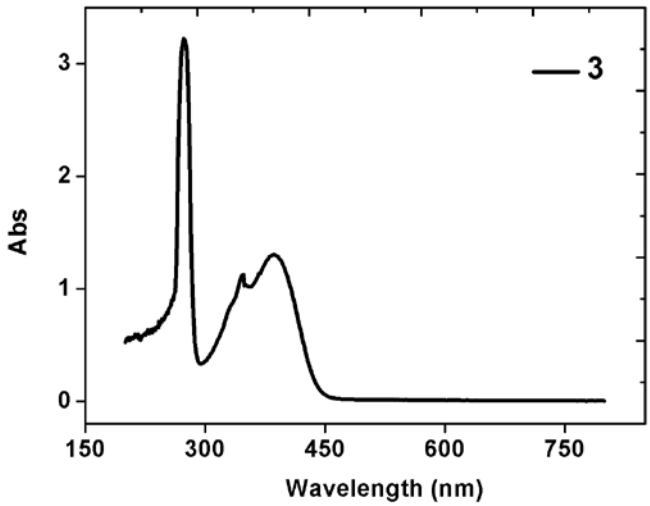

Figure S4. UV-visible absorption spectrum of complex **3** in DMF solution.

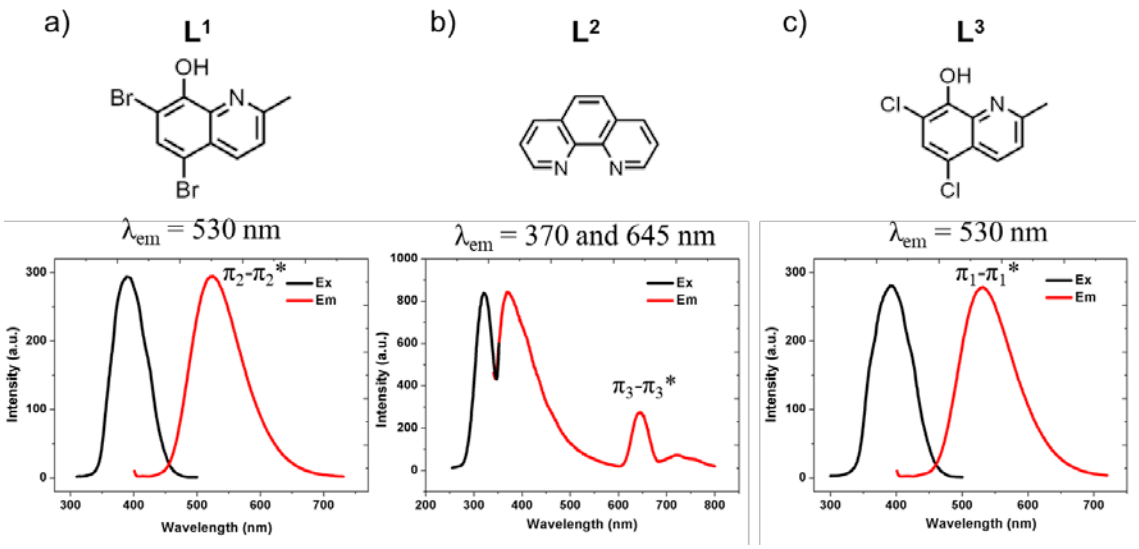

Figure S5. Ligands $\mathbf{L^1}$, $\mathbf{L^2}$, and $\mathbf{L^3}$ were fluorescently resolved in DMF.

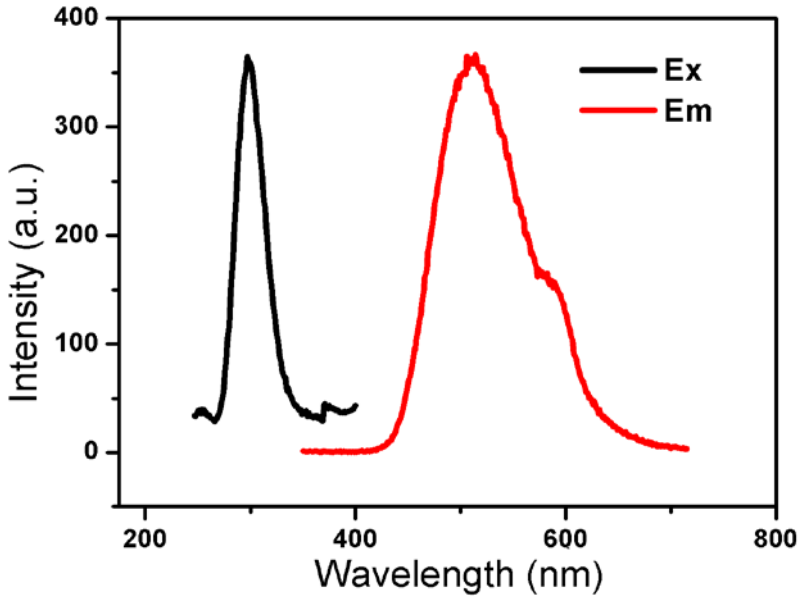

Figure S6. Fluorescence spectra of complex **3** in DMF solution.

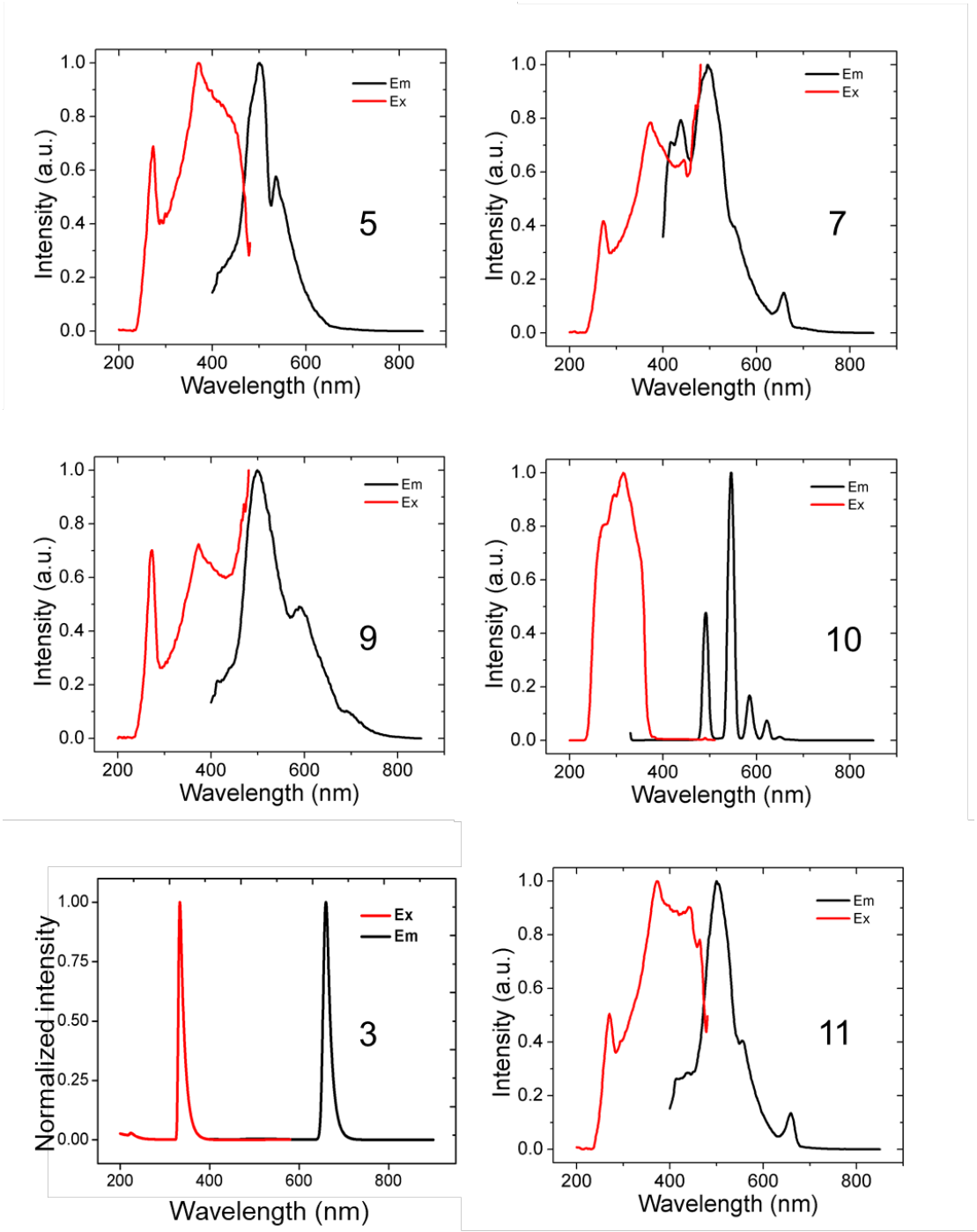

Figure S7. Complexes **3**, **5**, **9-11** solid fluorescence test pattern.

Table S4. Excitation (Ex) wavelength of complex **1-11**.

Compounds	Ex	Compounds	Ex
1	306 nm	2	320 nm
3	297 nm	4	325 nm, 420 nm

5	350 nm, 400 nm	6	373 nm
7	324 nm, 374 nm	8	332 nm, 418 nm
9	294 nm, 347 nm	10	339 nm
11	337 nm		

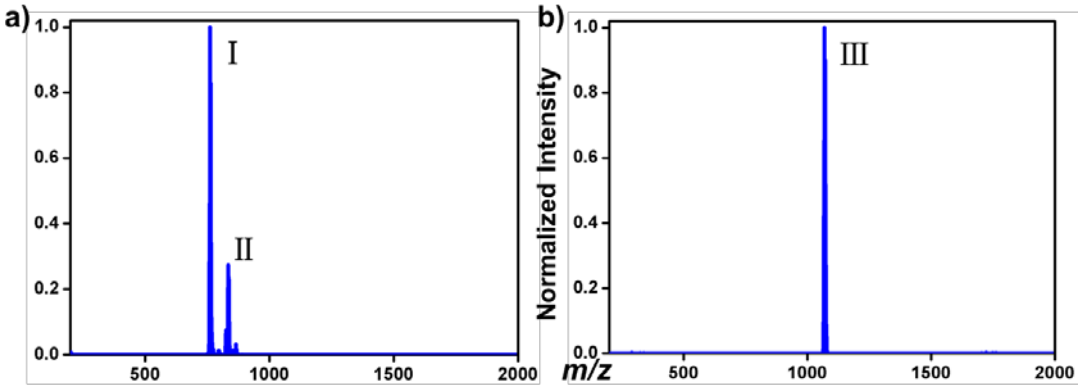

Figure S8. Positive ESI-MS spectra of **3** in DMF (In-Source CID 0 eV).

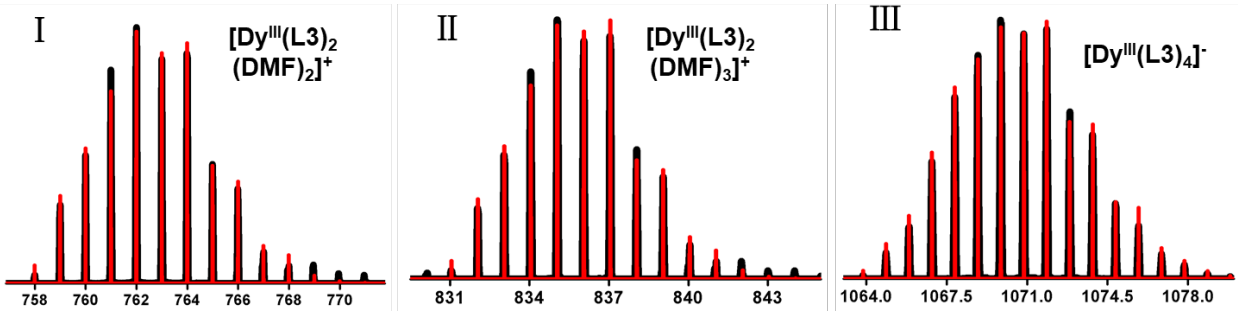

Figure S9. The superposed simulated and observed spectra of several species for **3**.

Table S5. Peak assignments of the ESI-MS spectrum of **3** (the In-source energy was 0 eV).

No.	Observed m/z	Calculated m/z	Fragments	Intensity
I	762.00	762.00	$[Dy^{III}(L^3)_2(DMF)_2]^+$	1.00
II	835.05	835.05	$[Dy^{III}(L^3)_2(DMF)_3]^+$	0.27
III	1069.85	1069.85	$[Dy^{III}(L^3)_4]^-$	1.00

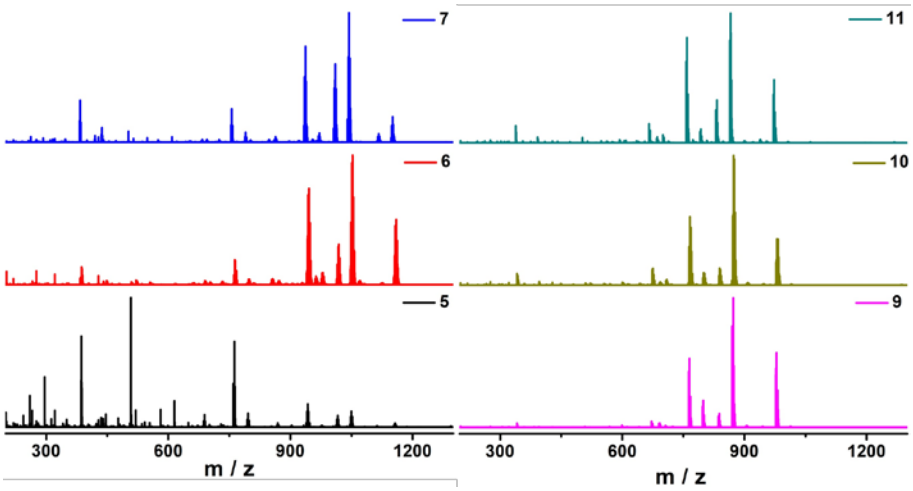

Figure S10. Positive ESI-MS spectra of **5-7** and **9-11** in DMF (In-Source CID 0 eV).

Table S6. Major species assigned in the ESI-MS of **5-7** and **9-11** in positive mode.

5			
Peaks	Relative Intensity	Obs. *m/z*	Calc. *m/z*
$[Ho(L^1)(DMF)_4]^{2+}$	0.700	386.51	386.51
$[Ho(NO_3)_2(DMF)_3]^{+}$	1	508.06	508.06
$[Ho(L^1)(NO_3)(DMF)_3]^{+}$	0.660	761.95	761.96
$[Ho(L^1)_2(DMF)_2]^{+}$	0.177	942.79	942.79
$[Ho(L^1)_2(DMF)_3]^{+}$		1015.85	1015.85
$[Ho(L^1)_2(L^2)(DMF)]^{+}$	0.122	1049.81	1049.81
6			
$[Er(L^1)(NO_3)(DMF)_3]^{+}$	0.191	762.96	762.96
$[Er(L^1)_2(DMF)_2]^{+}$	0.742	945.79	945.80
$[Er(L^1)_2(DMF)_3]^{+}$	0.311	1018.85	1018.85
$[Er(L^1)_2(L^2)(DMF)]^{+}$	1	1052.80	1052.80
$[Er(L^1)_2(L^2)_2]^{+}$	0.502	1159.82	1159.80
7			
$[Tb(L^1)(NO_3)(DMF)_3]^{+}$	0.257	755.95	755.95

$[Tb(L^1)_2(DMF)_2]^+$	0.740	936.78	936.78
$[Tb(L^1)_2(DMF)_3]^+$	0.602	1009.84	1009.84
$[Tb(L^1)_2(L^2)(DMF)]^+$	1	1043.80	1043.81
$[Tb(L^1)_2(L^2)_2]^+$	0.197	1150.81	1150.82
9			
$[Ho(L^3)_2(DMF)_2]^+$	0.532	765.00	765.00
$[Ho(L^3)_2(L^2)]^+$	0.207	798.96	798.96
$[Ho(L^3)_2(DMF)_3]^+$	0.106	838.05	838.05
$[Ho(L^3)_2(L^2)(DMF)]^+$	1	872.01	872.01
$[Ho(L^3)_2(L^2)_2]^+$	0.576	979.03	979.03
10			
$[Er(L^3)(NO_3)(DMF)_3]^+$	0.128	675.05	675.06
$[Er(L^3)_2(DMF)_2]^+$	0.528	766.00	766.00
$[Er(L^3)_2(L^2)]^+$	0.095	799.96	799.96
$[Er(L^3)_2(DMF)_3]^+$	0.129	839.05	839.05
$[Er(L^3)_2(L^2)(DMF)]^+$	1	875.00	875.00
$[Er(L^3)_2(L^2)_2]^+$	0.355	980.02	980.03
11			
$[Tb(L^3)_2(DMF)_2]^+$	0.811	758.99	758.99
$[Tb(L^3)_2(L^2)]^+$	0.105	792.95	792.96
$[Tb(L^3)_2(DMF)_3]^+$	0.329	832.04	832.05
$[Tb(L^3)_2(L^2)(DMF)]^+$	1	866.01	866.01
$[Tb(L^3)_2(L^2)_2]^+$	0.486	973.02	973.03

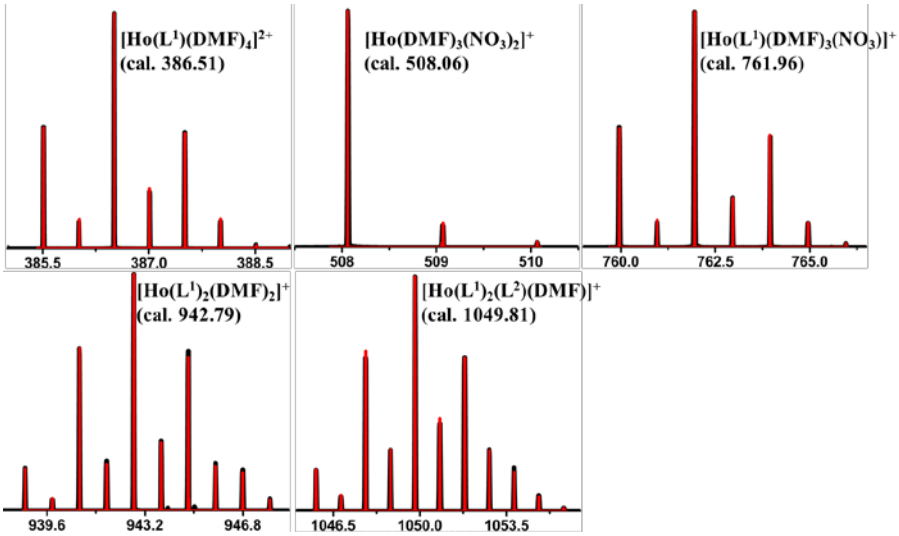

Figure S11. The superposed simulated and observed spectra of several species for **5**.

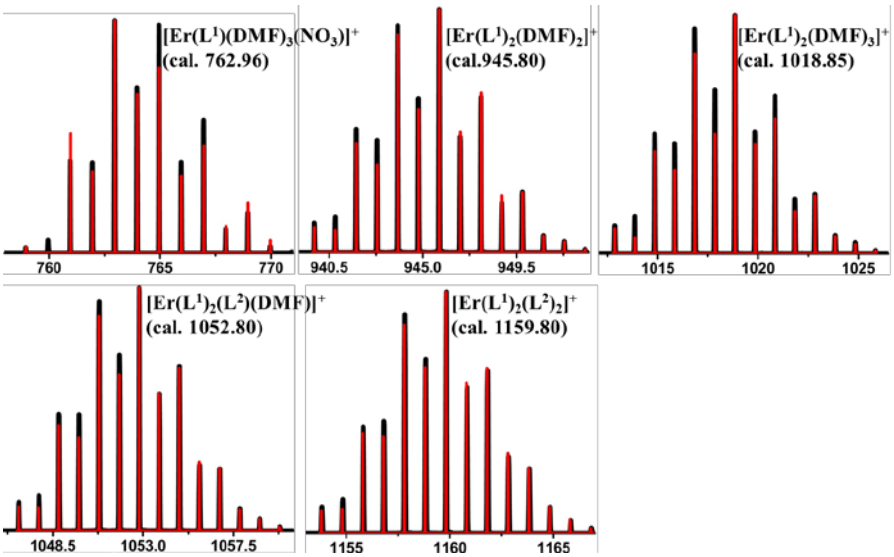

Figure S12. The superposed simulated and observed spectra of several species for **6**.

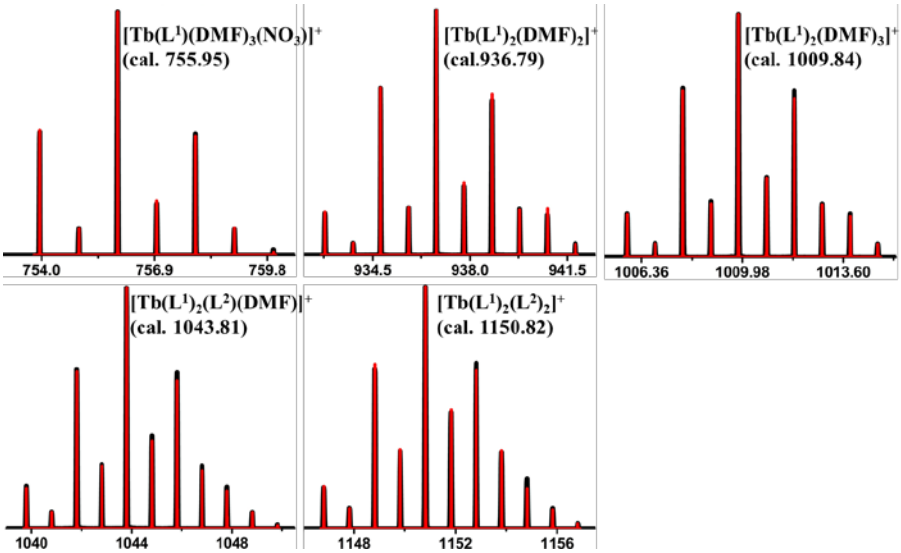

Figure S13. The superposed simulated and observed spectra of several species for **7**.

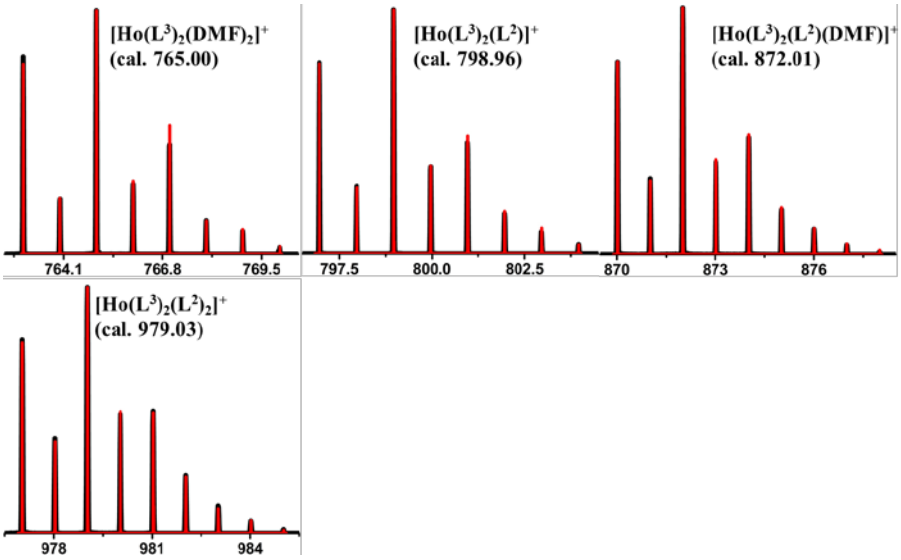

Figure S14. The superposed simulated and observed spectra of several species for **9**.

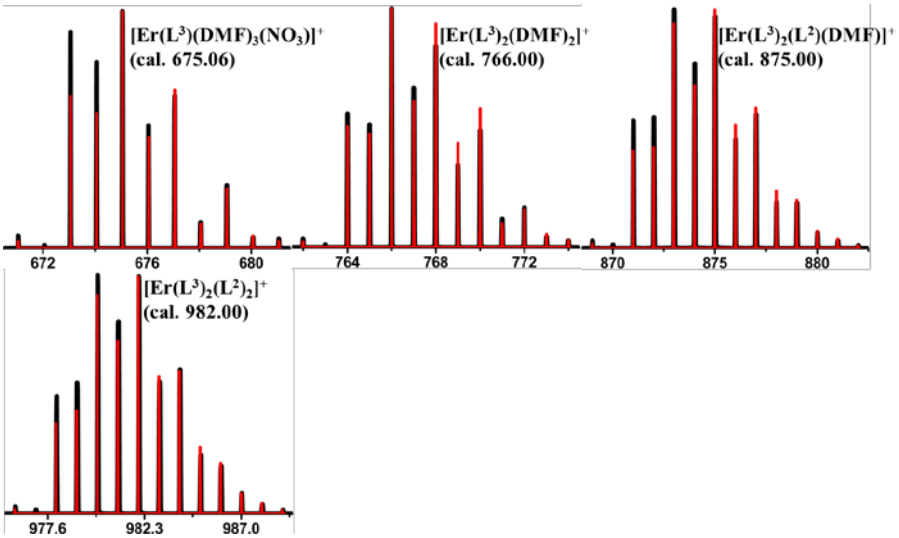

Figure S15. The superposed simulated and observed spectra of several species for **10**.

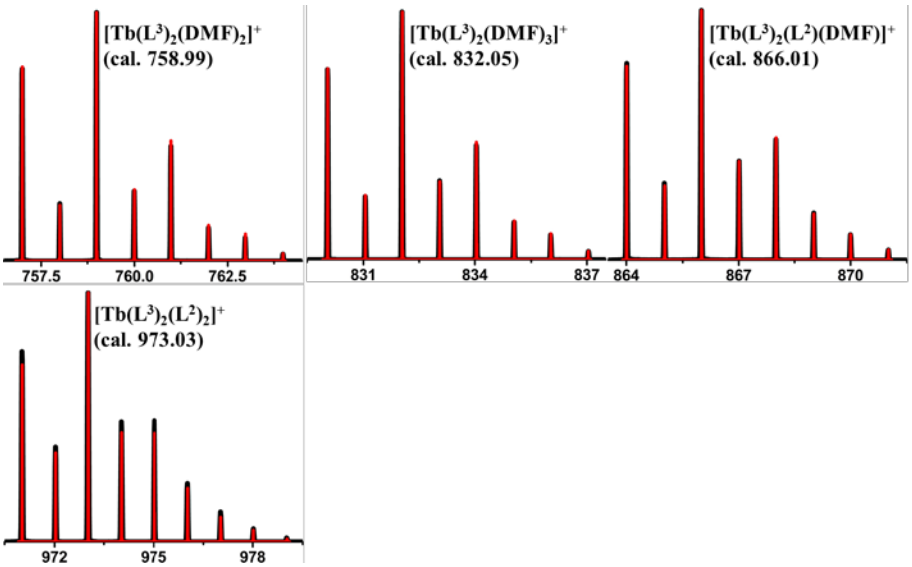

Figure S16. The superposed simulated and observed spectra of several species for **11**.

Negative mode ESI-MS：

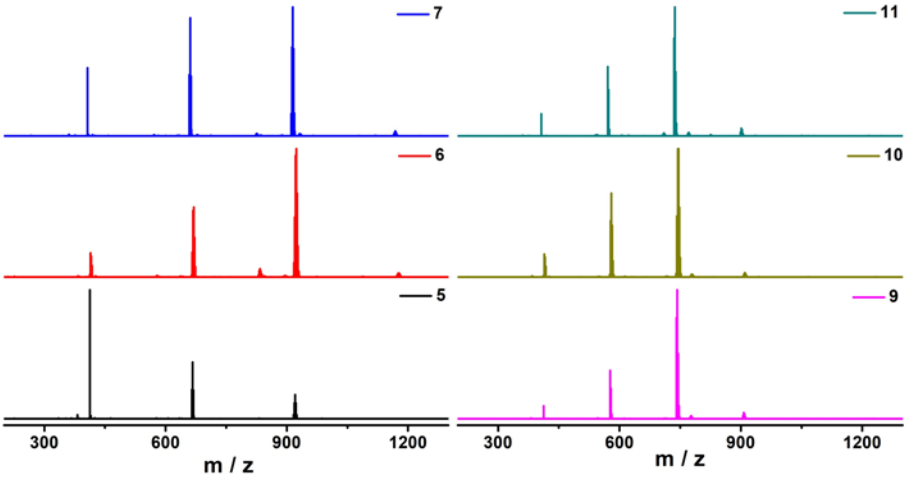

Figure S17. Negative ESI-MS spectra of **5-7** and **9-11** in DMF (In-Source CID 0 eV).

Table S7. Major species assigned in the ESI-MS of **5-7** and **9-11** in negative mode.

5			
Peaks	Relative Intensity	Obs. *m/z*	Calc. *m/z*
$[Ho(NO_3)_4]^-$	1	412.88	412.88
$[Ho(L^1)(NO_3)_3]^-$	0.442	666.77	666.77
$[Ho(L^1)_2(NO_3)_2]^-$	0.188	920.67	920.67
6			
$[Er(NO_3)_4]^-$	0.187	413.88	413.88
$[Er(L^1)(NO_3)_3]^-$	0.544	669.77	669.78
$[Er(L^1)_2(NO_3)_2]^-$	1	923.66	923.70
7			
$[Tb(NO_3)_4]^-$	0.526	406.88	406.88
$[Tb(L^1)(NO_3)_3]^-$	0.914	660.77	660.77
$[Tb(L^1)_2(NO_3)_2]^-$	1	914.66	914.66
9			
$[Ho(NO_3)_4]^-$	0.100	412.88	412.88
$[Ho(L^3)(NO_3)_3]^-$	0.377	576.88	576.88
$[Ho(L^3)_2(NO_3)_2]^-$	1	742.87	742.87

10			
$[Er(NO_3)_4]^-$	0.178	413.88	413.88
$[Er(L^3)(NO_3)_3]^-$	0.654	579.88	579.88
$[Er(L^3)_2(NO_3)_2]^-$	1	743.87	743.87
11			
$[Tb(NO_3)_4]^-$	0.167	406.88	406.88
$[Tb(L^3)(NO_3)_3]^-$	0.535	570.87	570.87
$[Tb(L^3)_2(NO_3)_2]^-$	1	736.87	736.86

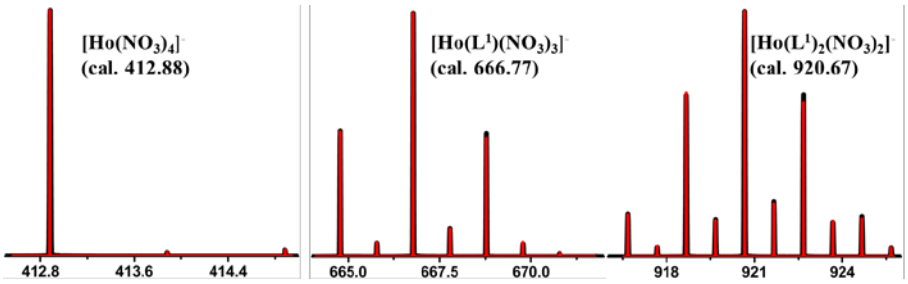

Figure S18. The superposed simulated and observed spectra of several species for **5.**

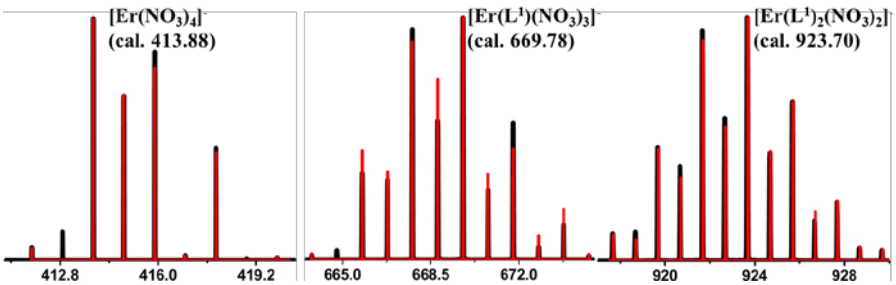

Figure S19. The superposed simulated and observed spectra of several species for **6**.

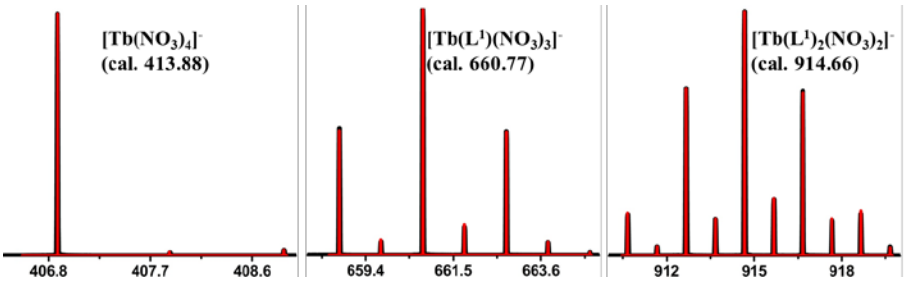

Figure S20. The superposed simulated and observed spectra of several species for **7**.

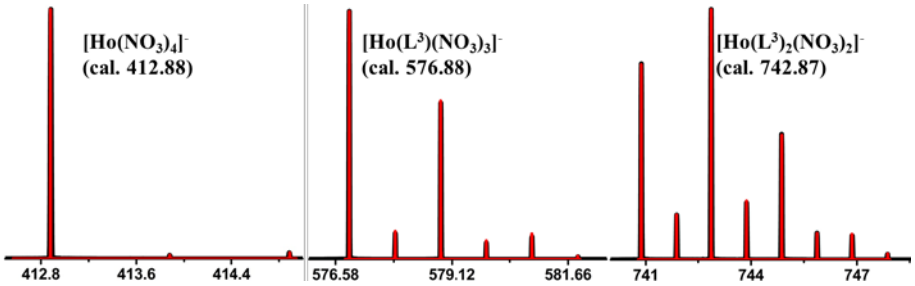

Figure S21. The superposed simulated and observed spectra of several species for **9**.

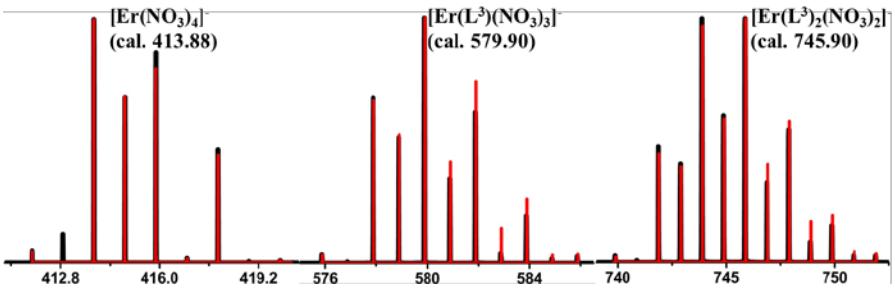

Figure S22. The superposed simulated and observed spectra of several species for **10**.

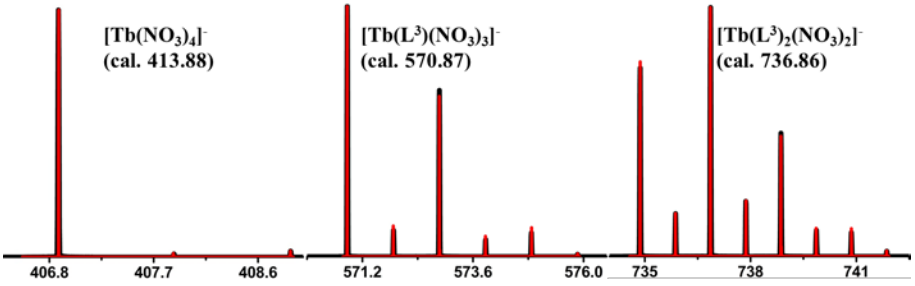

Figure S23. The superposed simulated and observed spectra of several species for **11**.

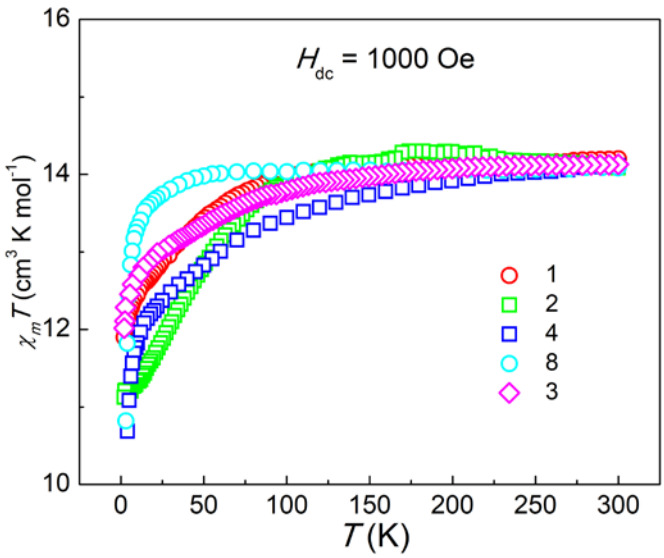

Figure S24. Temperature dependence of $\chi_m T$ for **1**-**4**, and **8**.

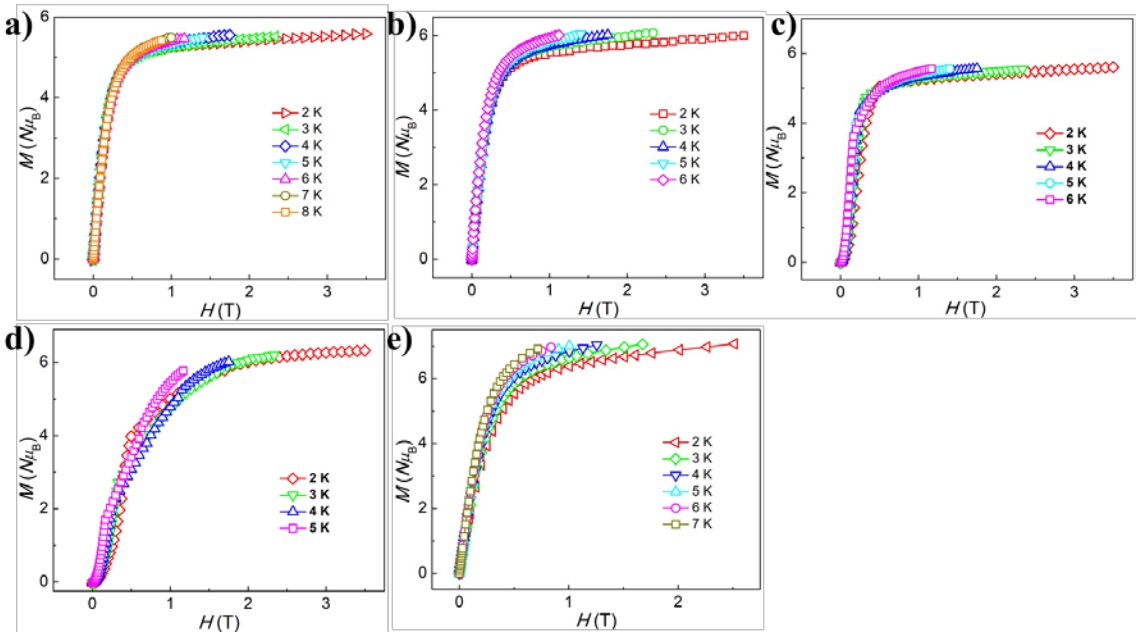

Figure S25. *M* vs. *H*/*T* plots for **1** (a), **2** (b), **3** (e), **4** (c), and **8** (d).

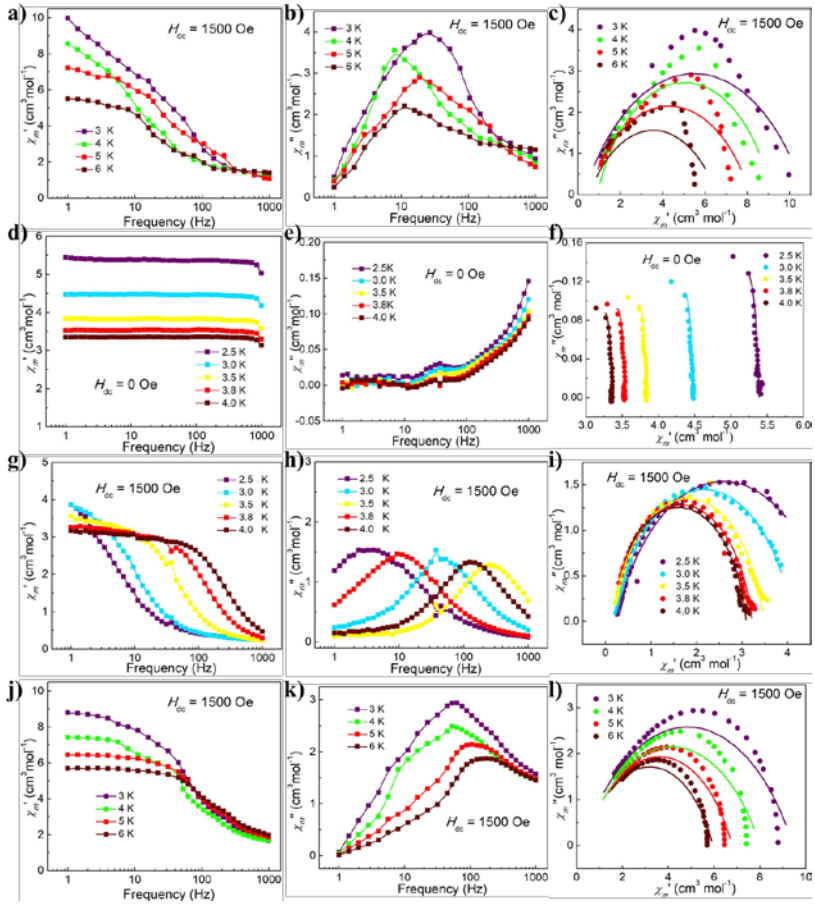

Figure S26. Variable-frequency dependent ac susceptibilities under 1500 Oe field for **1** (a and b), **2** (g and h) and **8** (j and k). Variable-frequency dependent ac susceptibilities under 0 Oe field for **2**. (d and e), cole-cole plots for **1** (c), **2** (i) and **8** (l) under 1500 Oe dc field, and cole-cole plots for **2** (f) under 0 Oe dc field.

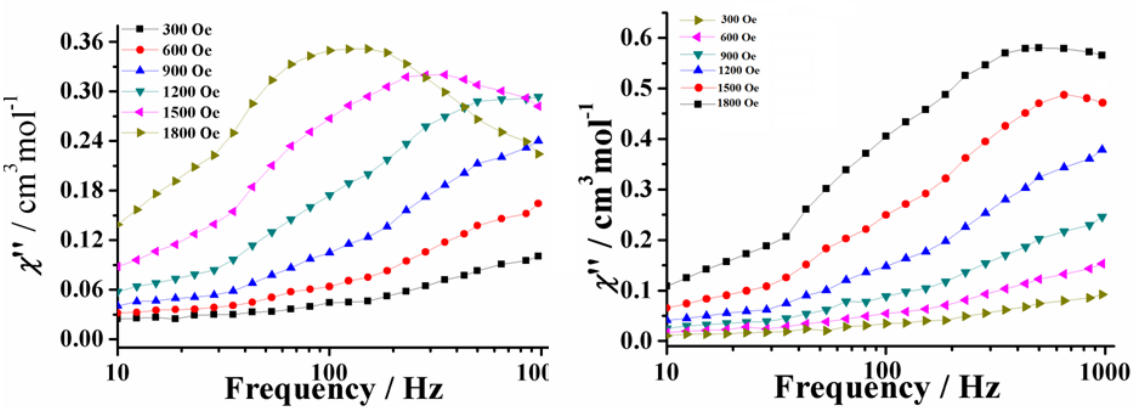

Figure S27. Out-of-phase susceptibility for **4** (left) and **8** (right) in various applied DC fields at 2 K.

Table S8. Selected parameters from the fitting result of the Cole-Cole plots for **4** and **8** under 0 Oe field.

	4			**8**		
Temp.(K)	τ	α	residual	τ	α	residual
2	1.28E-04	4.50E-03	5.56E-02	1.51E-04	1.17E-02	5.45E-02
3	1.23E-04	7.53E-03	2.34E-02	1.47E-04	1.20E-02	2.59E-02
4	1.17E-04	2.11E-02	1.70E-02	1.43E-04	2.01E-02	1.70E-02
5	1.15E-04	1.72E-02	1.01E-02	1.40E-04	2.66E-02	1.21E-02
6	1.11E-04	2.74E-02	7.47E-03	1.36E-04	3.29E-02	7.33E-03

Table S9. Selected parameters from the fitting result of the Cole-Cole plots for **4** and **8** under 1500 Oe field.

	4			**8**		
Temp.(K)	τ	α	residual	τ	α	residual
6	5.99E-04	2.07E-01	5.38E+00	4.02E-04	7.24E-01	1.36E+01
7	1.35E-02	2.57E-01	8.65E-02	5.98E-02	1.07E-01	1.00E+00
8	5.71E-03	2.60E-01	8.89E-02	2.77E-02	1.72E-01	4.52E-01
9	2.50E-03	2.64E-01	9.63E-02	1.13E-02	2.02E-01	3.57E-01
10	1.07E-03	2.55E-01	1.07E-01	4.50E-03	2.16E-01	3.73E-01
11	4.71E-04	2.42E-01	1.00E-01	1.84E-03	2.22E-01	3.87E-01
12	2.15E-04	2.31E-01	7.48E-02	7.61E-04	2.17E-01	3.65E-01
13	1.06E-04	2.32E-01	3.95E-02	3.34E-04	2.08E-01	2.58E-01
14	5.03E-05	2.79E-01	1.97E-02	1.56E-04	2.00E-01	1.47E-01
15	2.01E-05	3.77E-01	8.71E-03	7.88E-05	1.94E-01	6.46E-02